IEEE Access
Multidisciplinary | Rapid Review | Open Access Journal

Received 11 October 2023, accepted 23 October 2023, date of publication 31 October 2023, date of current version 6 November 2023.

Digital Object Identifier 10.1109/ACCESS.2023.3328798

RESEARCH ARTICLE

Leg Joint Angle Estimation From a Single Inertial Sensor During Variety of Walking Motions: A Deep Learning Approach

TSIGE TADESSE ALEMAYOH, (Student Member, IEEE), JAE HOON LEE, (Member, IEEE), AND SHINGO OKAMOTO

Department of Mechanical Engineering, Graduate School of Science and Engineering, Ehime University, Matsuyama, Ehime 790-8577, Japan

Corresponding author: Jae Hoon Lee (jhlee@ehime-u.ac.jp)

This work was supported in part by the Japan Society for the Promotion of Science (JSPS) KAKENHI under Grant JP22K04012.

This work involved human subjects or animals in its research. The authors confirm that all human/animal subject research procedures and protocols are exempt from review board approval.

ABSTRACT This study evaluates the capability of a single inertial sensor based joint angles estimation during four different walking patterns in an outdoor setting. The sensor was placed on the upper part of the tibia, which was chosen due to its large range of motion and minimal foot-ground impact. A Bi-LSTM (bidirectional long short-term memory) data-driven approach was used for joint angle estimation. The results showed smaller errors in intra-subject angle estimation compared to inter-subject, with an average MAE (mean absolute error) of 2.11° to 3.65°. The study suggests that deep learning approaches can effectively process data from a single IMU (inertial measurement unit) for accurate human motion monitoring, reducing the need for multiple sensors. Despite using only one sensor and four different walking patterns (zigzag, sideways, backward, and ramp walking), our method achieved similar results to previous studies that used single-motion activities. This study, conducted outdoors without instructing participants, is a step closer to real-world application, potentially providing insights into lower body biomechanics in physiotherapy, mobility improvement progress after surgery, and aiding in the development of personalized exoskeleton robots.

INDEX TERMS Deep learning, inertial sensor, joint angle estimation, pose estimation.

I. INTRODUCTION

The study and measurement of human motion and its characteristics is crucial for various scientific and medical applications. This includes healthcare applications where clinicians identify movement abnormalities, monitor rehabilitation progress, and pathological treatment effects [1], [2]. It is also essential to understand the impact of various disorders on a person's gait. For instance, musculoskeletal disorders such as knee and hip osteoarthritis can significantly alter a person's gait, leading to discomfort and reduced mobility [3]. Similarly, neurological disorders like Parkinson's disease can cause distinctive gait abnormalities, which can be used for early diagnosis and treatment planning [4]. It can also help neuroscientists to study the connection between the human brain and movement [5]. Additionally, it can be essential for sports experts and physiologists to investigate metabolic performances [6], injury prevention [7], [8], and athletic technique improvements [9], [10]. Moreover, the study of human motion can help engineers design user-friendly prosthetics, exoskeletons, and other assistive robots [11], [12], [13]. Beyond this, it can also be useful in virtual reality and animation applications [14]. This demonstrates how fundamental human motion study is for a wide range of applications, mainly in healthcare and science areas.

The associate editor coordinating the review of this manuscript and approving it for publication was Lorenzo Mucchi.

Different human motion analysis methods have been developed in recent years. These include human pose estimation [15], [16], [17], joint angle estimation [18], and gait analysis [19]. In this study, the focus will be on estimating lower-limb joint rotation angles. Joint angle estimation makes up one of the two main human gait parameter categories, whereas the other category comprises spatiotemporal parameters such as gait phase and step length [2]. Hence, leg joint angle estimation can be extended to human pose estimation, which in return could be utilized in computing leg kinematics and gait analysis. Hence, joint angles serve as a critical parameter in understanding human movement and diagnosing movement disorders [20].

Vision-based and non-vision-based human motion-data collection systems have evolved over the years in terms of size, performance, and mobility. Traditionally, vision-based sensor methods, particularly marker-based 3D motion capture systems, have been the industry standard human motion measurement and analysis methods [21]. The subjects were required to wear a special suit with markers attached to it. Despite its excellent accuracy in human motion measurement, it has its weak sides, which include being limited only to indoor spaces, affected by occlusions and ambient lighting, and high prices. On top of that, tight suits and several markers could make the wearer uncomfortable, which may alter the natural motion pattern [22]. To address the second issue, markerless pose estimation techniques surfaced in the human motion study area with the potential to facilitate human motion study without the need for special markers and suits. Even though marker-less and vision-based methods are limited to laboratory environments, they have emerged as significant pose estimation technologies in recent years. Some of the popular deep-learning-based pose estimation methods include OpenPose [17], AlphaPose [15], and DeepLabCut [16].

Marker-based motion measurement systems provide highly accurate measurements; however, they are expensive, require a controlled laboratory environment, and limit the naturalness of the movements. Non-vision wearable sensors, however, can be used in any environment, making them a promising tool for out-of-lab gait analysis. Recently, such sensors have brought a paradigm shift in human motion analysis, providing smaller sizes and better mobility. These sensors have attracted the attention of many researchers in the area as convenient motion measurement system techniques. Non-vision wearable sensors include sensors such as pressure sensors [23], [24], inertial sensors [18], [25], [26], [27], [28], and EMG (Electromyography) [29], [30]. Insole sensors can measure plantar pressure distribution during gait and can be used to estimate foot kinetics. However, insole sensors are limited to measuring only the forces acting on the foot and cannot provide information about the orientation or motion of other body segments. In contrast, EMG sensors measure muscle activity by detecting the electrical signals generated by muscle contraction. EMG sensors can provide information about muscle activation patterns during movement but cannot provide information about joint kinematics or kinetics. Inertial measurement units (IMUs), on the other hand, are advantageous over electromyography (EMG) and insole sensors in that they can provide more accurate and reliable data for human motion analysis as IMUs can measure the orientation, angular velocity, and acceleration of body segments, which can be used to estimate joint angles, joint torques, and joint power [31].

IMUs, which typically combine accelerometers, gyroscopes, and sometimes magnetometers, have emerged as a popular choice for wearable sensors due to their small size, low cost, and ability to capture high-frequency motion data [32]. The application of IMUs in the realm of biomechanics and rehabilitation is of paramount importance, particularly in the estimation of joint angles.

Despite the potential of IMUs, their application in joint angle estimation has been challenging owing to issues such as sensor placement, orientation, and integration drift [33]. Most existing studies used multiple IMUs placed on different body segments, which can be inconvenient and uncomfortable for users [28], [34]. Reference [34] employed two artificial neural network models to compute the extension/flexion angle of the knee joint and vertical ground reaction forces from three IMU sensors fixed on the pelvis and lower legs. Motion was performed on an instrumented treadmill in a laboratory. Resultantly, a mean RMSE (Root Mean Square Error) of $< 5°$ was attained for the knee flexion/extension angles. Reference [28] on the other hand, hired six participants to perform activities of daily living and sports exercises. They attached five inertial sensors to estimate the full-body joint poses. They achieved a joint position error of approximately 8 cm and a joint angle error of approximately 7°. Other similar studies, such as [26], [35], [36], [37], and [38], similarly utilized two or more IMU sensors for either knee angle estimation or including the ankle rotation angles. Particularly, [38], [39] adopted a model-based joint angle estimation using different algorithms such as Kalman filters. However, the common aspect of these studies is that they need two or more than two sensors to estimate one joint angle. If these methods were to be adopted for all the lower body joint angles, the number of sensors would be large. Additionally, the data used for the joint angle estimation was collected in an optical cameras-equipped controlled environment. This means subjects have to wear optical and inertial sensors together and perform motion activity in a certain indoor space. This could add complexity and measurement error to the system and discomfort to the subject.

Owing to the rapid development of artificial neural network models, researchers have recently begun to explore the use of a single IMU for joint angle estimation. A study by [25] used a CNN (Convolutional Neural Network) to estimate the sagittal plane one leg joint angles from 10 participants who performed running activity on a treadmill. It is not clearly explained why the authors chose to fix the IMU sensor on the foot rather than the waist or any part of the leg. They claimed to have obtained an RMSE of less than 3.5° and

6.5° in intra- and inter-participant scenarios, respectively, for sagittal plane angles. Similar work by [40] employed an LSTM (Long Short-Term Memory) to estimate the multi-joint leg joint angles from a low-frequency IMU sensor fixed on the lateral shank. Like [25], the ground-truth motion data was measured with an optical motion capture system. These studies show the promising potential of single inertial sensors in estimating leg joint angles. However, there is no consensus on where on the body the sensor should be placed. This was addressed in our previous work [27], where multiple candidate body parts were compared for multi-joint angle estimation. It was found that a single unit sensor attached to the shank resulted in better performance over other parts, the waist, thigh, and foot. These studies have only used one activity, either running on a treadmill or walking, to verify the possibility of estimating joint angles from a single IMU sensor.

In summary, the existing similar studies such as [25], [34], [35], and [40] have primarily focused on data collected in a controlled indoor motion (such as treadmills), single activity motion data, single leg joint angles estimation, and varying sensor placement. This study aims to extend this line of research by proposing a novel method for estimating both legs' hip and knee joint angles using a single IMU fixed on the shank of the right leg. By using motion data from four different activities, we have explored the possibility of lower limb pose estimation using a single unit of wearable sensor. This approach is motivated by the desire to minimize the number of sensors required, thereby enhancing the wearability and user comfort of the system.

Deep learning, a subset of machine learning characterized by the use of artificial neural networks with multiple layers, has shown great promise in handling the complexities of human motion data and improving the accuracy of joint angle estimation [25], [27], [40]. In this study, we leverage deep learning techniques to model the relationship between the IMU data and the joint angles, overcoming the limitations of traditional model-based methods. Our work is significant as it addresses a variety of walking activities, including backward walking, sideways walking, zigzag walking, and ramp walking. These activities represent a broad spectrum of daily life movements, enhancing the ecological validity of our approach. The use of a single IMU for joint angle estimation is a relatively new concept in the field of biomechanics. The majority of previous studies have relied on multiple IMUs, which can be cumbersome and uncomfortable for the subject. Our approach, which uses a single IMU fixed on the shank, offers a more user-friendly solution. This is particularly important in the context of long-term gait analysis, where user comfort and compliance are key factors for successful data collection. The proposed method could contribute mainly to the medical and robotics fields of study. In the medical area, particularly in rehabilitation, physiotherapists usually rely on their visual or complex indoor equipment for the evaluation of their patients. Attaching a single unit of sensor to patients and getting a numerical value of their joint movement would increase comfort to patients and insight to the clinicians. In addition, this method could contribute to the development of patient intention-aware exoskeleton robot design.

In this study, data from a single inertial sensor fixed below the knee of the right leg is used to estimate the sagittal plane joint angles of the leg, namely the hip and knee joints of both legs. Exceptionally, for sideways motion, the adduction/abduction hip joints and extension/flexion knee joints were obtained. The system overview is shown in Figure 1. The model was trained using the data from the shank IMU in a supervised fashion where ground truth joint angles were computed from all five sensors. During the inferencing phase, the trained model is used to estimate joint angles of unseen data, which are then visualized using a simulation. The contribution of this study is:

- Comprehensive joint angle estimation analysis of different walking activities, unlike previous studies, which only focused on a single motion type.
- The deep learning implementation on natural daily life motion patterns collected outdoors. This comprehensive analysis enhances the ecological validity of our approach and makes our results more applicable to real-world situations.
- By demonstrating the feasibility of using a single shank-mounted IMU for estimating hip and knee joint angles across different walking activities, we hope to pave the way for more accessible and comprehensive gait analysis solutions in the future. The results of our study have important implications for the field of biomechanics and rehabilitation.
- This study will contribute a bit towards the ongoing efforts of making wearable technology more practical and effective for human motion analysis.
- Lastly, the data collected in this study are published online for other interested researchers to replicate or work with new methods.

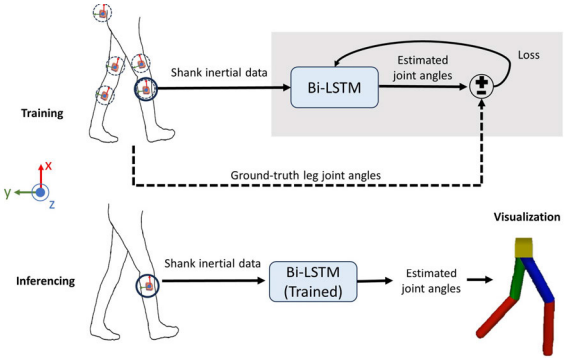

FIGURE 1. System overview.

II. MATERIALS AND METHODS

A. EXPERIMENT EQUIPMENT AND PROTOCOL

This study utilizes MTw Awinda sensors (hereafter referred to as inertial sensors) produced by Movella Inc., based in Nevada, USA. These sensors are wireless, compact, and

incorporate microelectromechanical system inertial sensors, making them ideal for real-time tracking of human movement. The inertial sensors provide accurate and synchronized data across all linked sensors, a critical feature for human pose estimation. The recorded data are saved on a computer with the help of proprietary software provided by Movella called MVN Analyze Pro. It is designed specifically for capturing and examining data from Xsens motion capture hardware systems, including MTw Awinda sensors. This software has the feature for real-time visualization of comprehensive body kinematic data. These include, but are not limited to, accelerometer data, gyroscope data, joint angles, segment orientations, and the center of mass.

FIGURE 2. Experimental setup and data collection.

Given that IMU sensors can be affected by drift errors and magnetized environments, it's crucial to validate and assess their performance before actual use. To validate this, studies by [41] and [42] evaluated the performance of the MTw Awinda sensor motion capture system in comparison to the gold-standard optical motion capture systems. After comparing with an 8-camera Qualisys optical motion capture system for 18 lower limb joints, [41] reported an RMSE of 3.2° to 10.1° for walking and 3.7° to 8.0° for static poses. The other study by [42] investigated the result of the MTw Awinda sensors against the Optotrak motion capture system for normal and stair walking. The authors obtained a mean joint angle estimation error of 1.38° to 6.69°. As an extra layer of evaluation, the performance of the inertial sensors was performed in this study as well. Even though the actual experiment was not in an indoor environment, the testing was done in an OptiTrack motion capture system-equipped laboratory room. A five-minute long data was collected using a rectangular rigid frame where reflective markers and an inertial sensor were mounted on it. The MAE (Mean Absolute Error) of the inertial sensor orientation was 1.45°, 1.66°, and 0.67° for the x, y, and z axes, respectively. Unlike this, our main data measurement was conducted in an outdoor setting where the environmental magnetic field is insignificant. Data were collected for about 10 minutes per subject to avoid potential long-term errors. As shown in Figure 2, data collection was carried out in an outdoor lawn space where there are no big structures that could potentially be a source of magnetic field. This was confirmed by measuring the magnetic norm variation of the experiment site, which remained within the ±0.2 range, a standard recommended by the manufacturer. Hence, the inertial sensor system is deemed reliable for the experimental and analytical requirements of this study.

In this study, fourteen healthy youth participants (11 male and 3 female) were recruited for the data collection. Informed consent was obtained from all subjects beforehand. The subjects have a demographic age of 24.5±5.7 years, height of 168.9±6.9 cm, and weight of 63.5±8.8 kg. Each participant provided written consent before the experiment. The motion data was collected by affixing seven inertial sensor units to the lower half of each participant's body. As illustrated in Figure 2, the sensors were attached to the part right above the pelvis bone, the lateral side of the femur of both legs, the upper part of the tibia of both legs, and the upper surface of the metatarsals of both feet. These sensor positions are recommended by the sensor manufacturer, considering the effect of soft tissue and skin motion artifacts. The sensors are then firmly fixed to the body using non-slip Velcro tape straps.

Once the subjects confirm that they feel comfortable with the attachments, calibration is carried out. The calibration procedure was performed as follows. First, anthropometric information such as height and shoe size were recorded. After sensors are attached to their corresponding position, the subject stands still in an ''N-pose'' for three seconds. This is followed by a 10-second circular and slow walking motion. This completes the calibration process, and data recording can be conducted afterward.

Subjects were then instructed to walk naturally, in any direction, altering their pace to slow, normal, or fast at varying step lengths. The interpretation of the motion pace and stride length was left to the subjects' intuition. Each subject performs four different motion activities: backward, sideways, zigzag, and ramp walking. Each activity was assigned 10 minutes, which totals 40 minutes per subject for all activities. Calibration was done only once, at the beginning, to avoid any placement errors. An Awinda Station manages the process of receiving synchronized data from all sensors, which are connected wirelessly through a radio protocol. The Awinda station is serially connected to an LG Gram 11th Gen Intel® Core™ i7 computer to save the motion data. The Awinda station antenna supports wireless communication up to a 50-meter radius, making the data collection process convenient. Motion data were collected at 100 Hz of sampling frequency. Figure 3a and Figure 3b provide a visual representation of the shank inertial data and joint angles data.

B. DATASET PREPARATION

Different motion information can be exported as CSV files using the MVN Analyze Pro software. This data encompasses both the input data, which consists of triaxial linear acceleration and angular velocity data, and the output data, which includes joint angles data. The joint angles data is composed of the four extension/flexion angles of the hip and the knee for both legs, as shown in Figure 4.

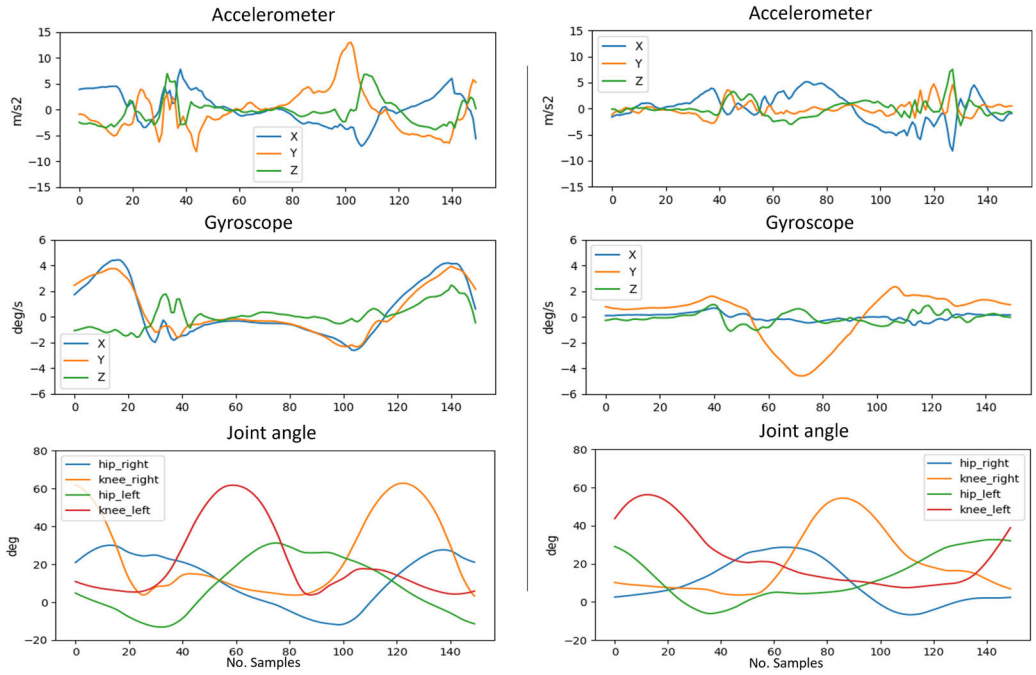

FIGURE 3. Raw inertial and joint angle data, zigzag walking (left) and backwards walking (right).

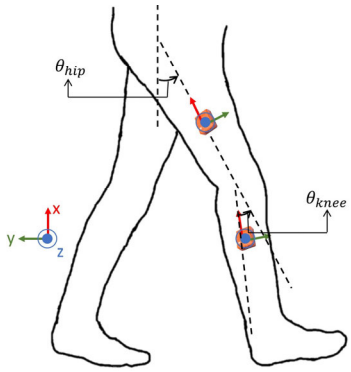

FIGURE 4. Leg joint angles; the hip and knee joints.

For effective deep-learning training, it is crucial to segment the raw time-series motion data into smaller datasets. To accomplish this, we adopted a sampling window of width of 50 and stride of 10, corresponding to 0.5 seconds of data, for the preparation of the datasets. The decision to use a width of 50 was made after conducting a comparative analysis among widths of 20, 50, and 100 for joint angle estimation training for a single subject. The results demonstrated that the sampling window with a width of 50 yielded better results. Datasets are found at https://github.com/tsgtdss583/multiActivities/tree/main.

The process of preparing and segmenting the data for deep learning training is a critical step in our study. It allows us to effectively train the neural network and evaluate its performance using a separate testing dataset. In our previous study [27], we discovered that the use of the sensor affixed to the tibia (shank) for joint angle estimation during straight walking yielded more accurate results compared to other sensors. The use of the sensor affixed to the tibia has proven to be effective in our previous study [27], and we continue to utilize this approach in our current research as well. Consequently, in this study, the inertial data from the tibia of the right leg was selected as the input for the neural network. The input dataset is shaped into a 50 $\times$ 6 array, where 50 represents the sampling window size and 6 accounts for the 3-axis accelerometer data and the 3-axis gyroscope data. In addition, the output data is prepared in a 4 $\times$ 1 vector format representing the four joint angles. The estimation problem in this study is solved by taking the previous 50 samples of tibia inertial data to compute the current leg joint angles.

The training was conducted using data from thirteen subjects, while the data from one additional subject was used as a testing dataset for the trained neural network. It is important to note that joint angle values can vary significantly between subjects. To illustrate these differences, boxplots of each subject's joint angles for backward motion are shown in Figure 5. As can be seen from the boxplots of the Figure, the variability of the data is visible more on the hip joint angles than the knee joint angles. This illustrates the variability in hip movements during walking motions. One reason for the variation of hip joint angles but not significant variation in knee joint could be that the hip joint is a ball-and-socket joint, which allows for a wide range of motion, including flexion, extension, abduction, adduction, internal rotation, and external rotation while the knee joint is a hinge joint which allows movement primarily in one plane. The hip joint

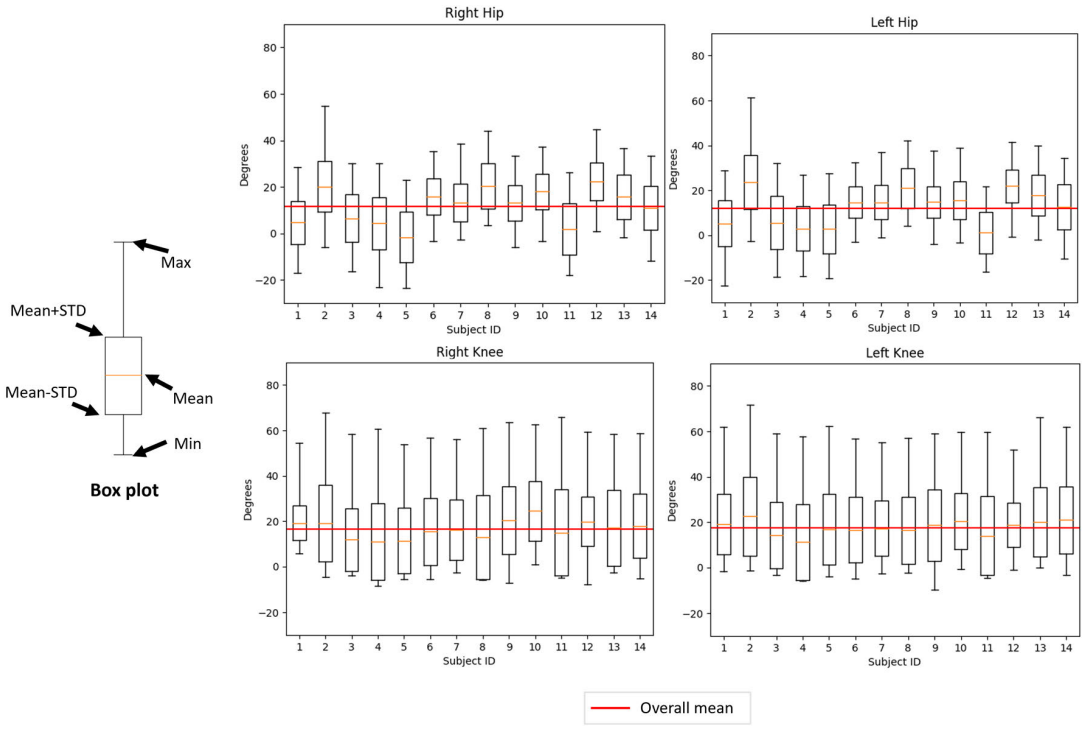

FIGURE 5. Boxplot of the four joint angles (backward walking). STD stands for standard deviation.

is not significantly constrained in its movements; however, the knee joint is more constrained in compared to the hip joint. Specifically, the knee joint is constrained in its extension, meaning it cannot extend beyond a certain point (usually 0 degrees or straight). Furthermore, the variability in the hip joint angles could be attributed to the differing inclinations of each subject's torso. For example, a subject with an upright posture will exhibit a smaller hip extension angle in contrast to a subject with a torso leaning forward. This variation arises from our assumption of a uniform straight torso for all subjects.

C. DEEP LEARNING MODEL

Bidirectional Long Short-Term Memory networks (Bi-LSTMs) have emerged as a powerful tool for deep learning on time-series data, owing to their unique architecture and capabilities [43]. Bi-LSTMs are an extension of traditional Long Short-Term Memory (LSTM) networks, a type of recurrent neural network (RNN) that effectively addresses the vanishing gradient problem, which is a common issue in training traditional RNNs [44]. LSTMs introduce the concept of a memory cell that can maintain information in memory for long periods of time, making them particularly suitable for tasks that involve dependencies over different time steps.

Bi-LSTMs enhance the capabilities of LSTMs by introducing a second hidden layer in the opposite direction to the original layer. This means that each output layer can get information from past (backward) states and future (forward) states simultaneously. This bidirectional structure allows the model to have access to both past and future contexts, which is a significant advantage when dealing with time-series data where future context can provide valuable information for the current state [45].

The efficacy of Bi-LSTMs in the context of joint angle estimation has been previously demonstrated, as evidenced by the study conducted by [18]. Their excellent performance in this specific problem domain has led us to adopt Bi-LSTM as the neural network model for deep learning in our current study.

The architecture of our chosen model is depicted in Figure 6. It comprises a 256-unit Bi-LSTM, which operates with a time step of 50, followed by four fully connected layers. This structure is designed to effectively process the time-series data and capture the temporal dependencies inherent in joint angle estimation. Given that the target output angle values can span from positive to negative, a linear activation function was chosen as an activation function of the last layer. This is due to the nature of linear activation functions, which do not constrain the output to a specific range, thus allowing for both positive and negative output values. This is particularly important, as it ensures that the full range of possible joint angles can be accurately represented by the model's outputs.

The training of the neural network was conducted utilizing a specific set of hyperparameters, which were determined through a process of trial and error to optimize the network's performance. These hyperparameters included a dropout rate of 0.3, a batch size of 32, and a training period of 30 epochs. The optimization algorithm employed was the

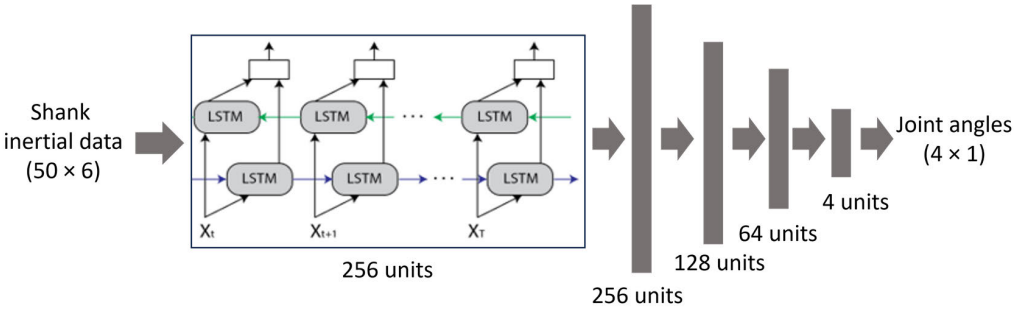

FIGURE 6. The Bi-LSTM model.

TABLE 1. Intra-subject models' MAEs, RMSEs, and Pearson's correlation coefficients.

Subject ID	Right hip (°)			Right knee (°)			Left hip (°)			left knee (°)			Average (°)	
	MAE	RMSE	ρ	MAE	RMSE	ρ	MAE	RMSE	ρ	MAE	RMSE	ρ	MAE	RMSE
Sub 1	1.84	2.52	0.97	2.05	2.84	0.98	2.41	3.43	0.96	4.35	6.45	0.93	2.66	3.81
Sub 2	2.90	3.82	0.96	3.58	5.25	0.96	3.38	5.10	0.94	4.73	6.99	0.93	3.65	5.29
Sub 3	2.13	3.08	0.96	2.72	3.97	0.97	2.88	4.68	0.92	4.07	6.18	0.93	2.95	4.48
Sub 4	2.40	3.44	0.97	3.06	4.33	0.98	2.87	4.17	0.95	3.93	5.87	0.95	3.07	4.45
Sub 5	3.13	4.98	0.93	2.85	3.79	0.97	3.33	4.98	0.93	3.84	5.59	0.94	3.29	4.84
Sub 6	2.73	4.01	0.93	2.76	3.65	0.98	3.02	4.37	0.91	3.81	5.34	0.95	3.08	4.34
Sub 7	1.80	2.71	0.97	2.05	2.92	0.98	1.93	3.02	0.97	2.64	4.13	0.95	2.11	3.20
Sub 8	1.80	2.64	0.98	1.95	2.69	0.99	2.23	3.33	0.97	2.91	4.84	0.96	2.22	3.38
Sub 9	2.13	3.31	0.94	2.80	4.10	0.96	2.46	3.72	0.92	3.52	5.22	0.94	2.73	4.09
Sub 10	2.22	3.39	0.95	2.40	3.72	0.96	2.52	3.77	0.94	3.09	4.68	0.93	2.56	3.89
Sub 11	2.09	2.78	0.97	2.44	3.24	0.98	2.30	3.30	0.95	4.14	6.16	0.93	2.74	3.87
Sub 12	1.74	2.36	0.98	2.27	3.09	0.98	2.21	3.18	0.97	2.90	4.07	0.96	2.28	3.18
Sub 13	2.92	5.39	0.93	1.93	2.86	0.99	2.86	4.78	0.94	2.81	4.37	0.97	2.63	4.35
Sub 14	2.48	3.58	0.95	2.49	3.49	0.98	3.14	4.47	0.93	4.07	6.42	0.92	3.05	4.49

Adam optimizer, which was trained using the Huber loss function. Besides the dropout layer, L2 norm regularization was also implemented on all the weights.

The Huber loss function, also known as the Smooth Mean Absolute Error, is a robust regression loss function that combines the advantages of the MAE and the Mean Squared Error (MSE). The mathematical representation of the Huber function is provided in Equation (1). The unique characteristic of the Huber loss function is its ability to reduce the impact of outliers on the training process [46].

$$\mathbf{L}_{\delta}\left(\boldsymbol{y}, \varphi\left(\boldsymbol{x}\right)\right) = \begin{cases} \frac{1}{2}(\boldsymbol{y} - \varphi\left(\boldsymbol{x}\right))^2, & for\ |(\boldsymbol{y} - \varphi\left(\boldsymbol{x}\right))| \leq \delta \\ \delta\,|(\boldsymbol{y} - \varphi\left(\boldsymbol{x}\right))| - \frac{1}{2}\delta^2, & otherwise \end{cases} \tag{1}$$

In this equation, $\boldsymbol{y}$ represents the actual joint angles, which are obtained from the MVN Analyze Pro. On the other hand, $\varphi\left(\boldsymbol{x}\right)$ symbolizes the neural network that takes the input vector $\boldsymbol{x}$. The hyperparameter δ is utilized to choose one of the functions in equation (1). The selected value for δ in this study is 1.

III. RESULTS

In this section, the results of the deep learning model will be discussed in detail. The data from the fourteen subjects were used to train two models, one for intra-subject analysis and another for inter-subject analysis. Both models were Bi-LSTM networks of similar architecture but trained with different datasets.

A. INTRA-SUBJECT

In this part, the four-motion data of a single subject are used to train a neural network. Hence, fourteen separate neural network models were prepared per subject. The dataset of each subject was divided into training, validation, and testing datasets at 77%, 13%, and 10% ratios, respectively. The results of the training are reported in Table 1 in terms of the MAE, RMSE, and Pearson's correlation coefficient (ρ) metrics. The results in the table are obtained after each trained intra-subject model was given the 10% testing dataset as input. The MAE metric is easier to understand as it represents the exact error of the results compared to the reference joint angle values. However, it is more common to use metrics such as RMSE and Pearson's correlation coefficient. Pearson's correlation coefficient is a statistical

TABLE 2. Inter-subject model's MAEs, RMSEs and Pearson's correlation coefficients.

Test dataset	Right hip (°)			Right knee (°)			Left hip (°)			left knee (°)			Average (°)		
	MAE	RMSE	ρ	MAE	RMSE	ρ	MAE	RMSE	ρ	MAE	RMSE	ρ	MAE	RMSE	ρ
Ramp	3.51	4.43	0.91	3.38	4.20	0.97	4.76	5.63	0.85	5.71	7.57	0.91	4.34	5.46	0.92
Backward	4.45	5.68	0.85	3.05	4.24	0.95	5.01	6.14	0.80	4.91	6.78	0.88	4.35	5.71	0.87
Sideways	3.95	5.07	0.74	4.31	5.10	0.73	3.50	4.30	0.80	6.29	7.49	0.52	4.50	5.49	0.70
Zigzag	2.95	3.78	0.94	3.10	3.91	0.97	4.13	4.93	0.87	4.67	6.47	0.93	3.71	4.77	0.94
All combined	3.69	4.76	0.87	3.45	4.37	0.95	4.37	5.30	0.83	5.38	7.09	0.89	4.22	5.38	0.90

measure that calculates the strength of the relationship between the relative movements of two variables. The values of the Pearson correlation coefficient are always in the range of -1 to $+1$. The correlation coefficients represent the linear correlation between the predicted and ground-truth joint angle values, where $+1$ indicates a perfect positive correlation, -1 indicates a perfect negative correlation, and 0 indicates no correlation at all. Hence, the ρ values range from 0.91∼0.99 which indicates a strong correlation between the predicted and ground-truth joint angles. This is supported by the average of MAE and RMSE over the number of joints, which range from 2.11° ∼3.65° and 3.18° ∼5.29° respectively. It is important to note that each subject's data does not include a single motion data of the subject, as in many other studies, but a combination of four motion data. Even though it is one subject's data, it is partly diversified due to the different motions. Therefore, this is a promising result in understanding the leg kinematics of humans during different locomotive activities.

B. INTER-SUBJECT

In this model, all fourteen subjects' data were combined and utilized for training and testing. First, the data from the thirteen subjects were combined into one dataset, which was later used as a training and validation dataset with a 77% and 13% ratio. The remaining 10%, corresponding to one subject's data, were subsequently used as a testing dataset to evaluate the performance of the trained network. As discussed in section II-B, each subject has a unique way of locomotion. Hence, we can consider in inter-subject training; there are $14 \times 4 = 56$ motion varieties. On top of that, the subjects are not accustomed to backward and sideways motions in their daily life. This has made the subjects perform those activities in an irregular and non-uniform way. Particularly, subjects struggle to keep a uniform knee movement during sideways walking. The effect of such non-uniform motions is evident in the network's performance, as shown in Table 2. The MAE and ρ of backward and sideways motions are lower when compared to the other two. The main movement of the sideways motion is manifested on the hip, and the results for the hip joints are better than the knee joints. Generally, the model attained an average MAE and RMSE over the four joints of 3.71° ∼4.50° and 4.77° ∼5.71° respectively. This average was computed as the average of the four joints' MAE values of each motion type. By combining all four testing datasets into one, the model MAE was calculated. These results are 3.69°, 3.45°, 4.37°, and 5.38° associated with the right hip and knee and the left hip and knee, respectively. The joint angle errors of the right leg are lower compared to those of the left leg. It is the same with the RMSE values shown in the table. This discrepancy is attributed to the sensor's placement on the right tibia, which allows it to directly capture the motion of the right leg but not the left leg. However, given the periodic nature of the motions, the model can infer the orientation of the left leg relative to the right leg. Lastly, the overall Pearson's correlation coefficient is 0.90, indicating a strong agreement between the two values was achieved.

The outcomes derived from the inter-subject model are illustrated in various graphical formats in the figures shown. Figure 7 presents a box plot representation of the four joint angles derived from the test dataset associated with ramp walking. The box plot corresponding to the test dataset from ramp walking is highlighted by a red rectangular box. A notable characteristic observed in these results is the convergence of the mean value of the predicted joint angles towards the overall mean of the joint angles. This particular trait is consistently observed across the other four types of motion.

IV. DISCUSSION

Figure 8 provides a segment of the graphical comparison between the actual (ground-truth) joint angles and the predicted joint angles, represented by solid and broken lines, respectively. These graphs specifically pertain to the predicted left hip joint angle of the four types of motion. The predicted angles exhibit a waveform pattern that closely mirrors that of the actual joint angles. However, slight discrepancies are observed in the phase alignment for the bottom two graphs, and amplitude errors are noticeable at the peaks and valleys (during full flexion and extension) of the upper two graphs.

The phase misalignment may be attributed to the gait speed, where most subjects might have performed the motions at different gait paces. This could potentially result in an imbalance in the dataset prepared. The second discrepancy could be associated with the range of joint rotation among the subjects. It is obvious that people have different ranges

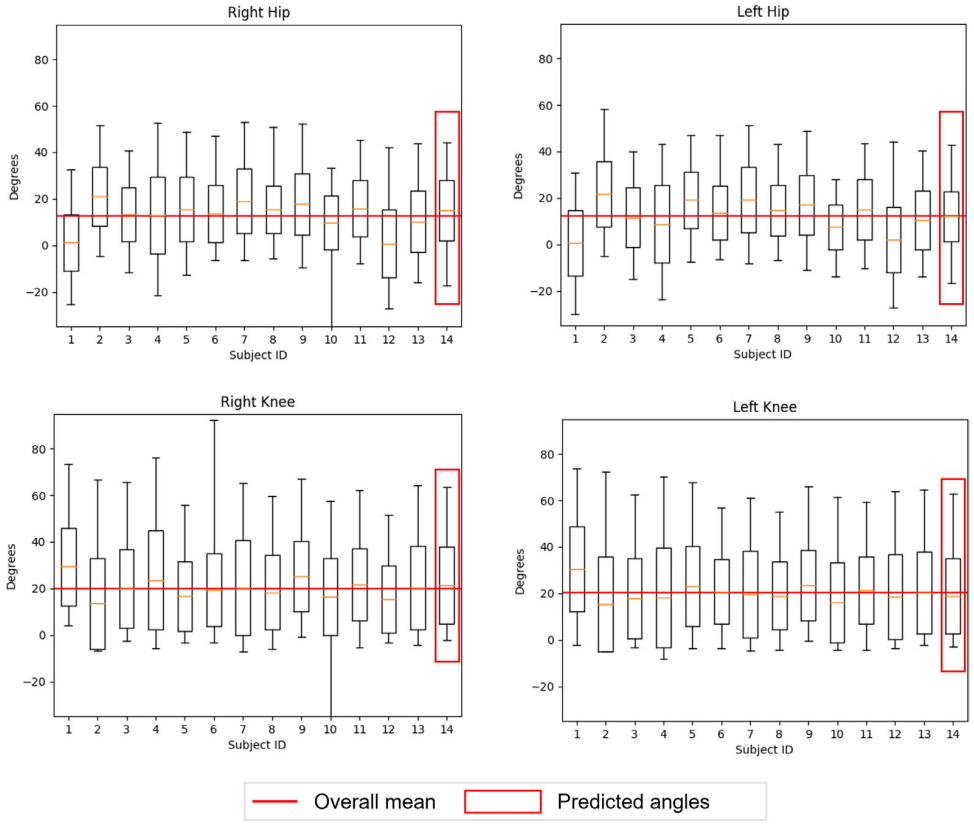

FIGURE 7. Boxplot of the predicted joint angles in comparison to the other thirteen subjects' ground-truth data used for training (ramp walking).

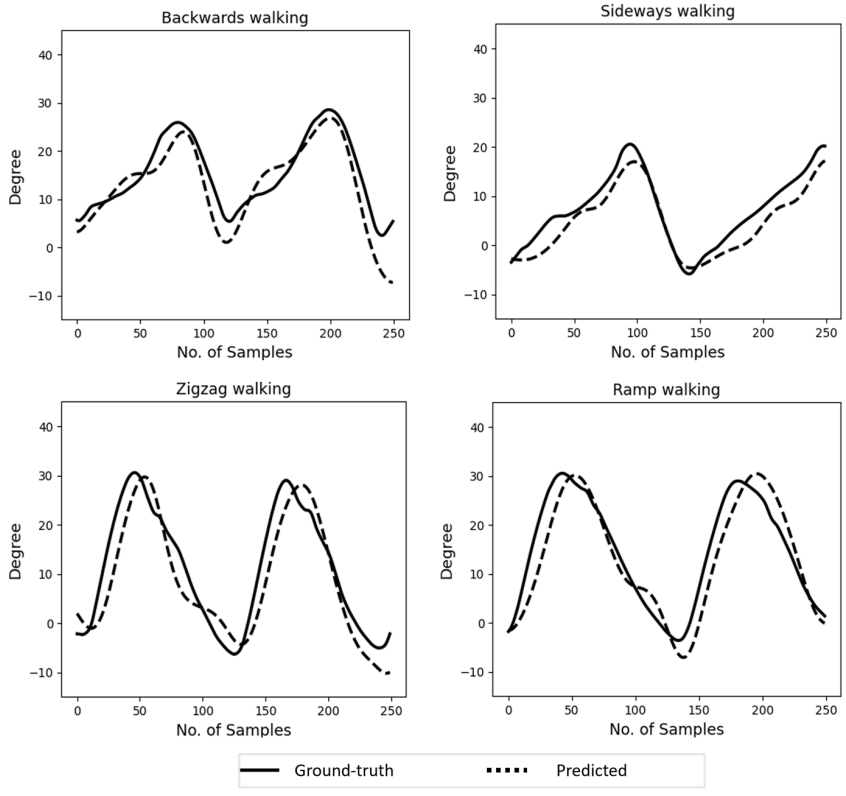

FIGURE 8. Graphical representation of the ground truth and the predicted left hip joint angle across the four motion patterns.

FIGURE 9. Comparison of the actual testing subject motion and simulation of the predicted joint angles. from left to right: backwards walking; sideways; ramp walking; zigzag walking.

TABLE 3. Comparison of our study with other previous studies.

Paper	[34]	[25]	[40]	[35]	Ours
Data collection	Treadmill	Treadmill	Indoor (5m)	Treadmill	Outdoor
Motion type	Running	Running	Straight walking	Level walking	Zigzag walking Backward walking Sideways walking Ramp walking
Inertial sensors	3	1	1	2	1
Number of subjects	8	10	30	1	14
Method	Data-driven	Data-driven	Data-driven	Data-driven	Data-driven
Intra/ Inter-subject	Yes	Yes	Yes	No	Yes
Joint angles	Right knee Left knee	Left hip Left knee Left ankle	Right hip Right knee Right ankle	Knee Ankle (Subtalar Talocrural)	Right hip Right knee Left hip Left knee
RSME Result (inter-subject)	4.66~19.47 5.88~19.11	5.6 6.5 4.7	6.19 7.00 4.35	MAE (intra-subject) 2.37 1.69 1.37	4.76 4.37 5.30 7.09

of joint rotation which results in different stride lengths and different paces. This is one of the inevitable sources of errors for such systems as deep learning algorithm outcomes often gravitate towards larger datasets of similar features. The features in this case are either smaller or larger rotation ranges.

Regarding the estimation error of joint angles, the intra-subject error was smaller than the inter-subject error, with an average MAE of 2.11° ∼3.65° and RMSE of 3.18° ∼5.29°. However, the MAE was larger for the inter-subject case, measuring an MAE of 4.22°, RMSE of 5.38° with a ρ of 0.90. This discrepancy can be attributed to the diversity of the data in terms of gender, speed, step length, and individual walking patterns, all of which influenced the results. A higher ρ value here indicates a stronger agreement between the actual and predicted joint angles. Additionally, the left knee exhibited the poorest results compared to the other three joints, as reported in Table 1 and Table 2, likely due to the sensor's placement being distant from the left knee joint, which is fixed on the upper tibia bone of the right side.

Furthermore, the predicted joint angles were simulated using a two-legged character in MATLAB Simulink, as depicted in Figure 9. The direction of motion is indicated by an arrow while the right and left legs are depicted in orange and green colors, respectively. These results were obtained from a subject whose motion data were not used during the training.

The above findings hold significant promise for the field of gait analysis and pose estimation. While motion analysis

requiring high precision and detailed information may pose challenges given the current results, it is noteworthy that various gait events can be easily identified and measured using the single inertial sensor unit affixed below the knee joint. More importantly, the results for intra-subject analysis outperform those of inter-subjects, suggesting the potential for personalized gait and general motion analysis applications.

Data were collected from fourteen participants who performed four dynamic walking motions: backward, sideways, zigzag, and ramp walking. A data-driven approach, based on Bi-LSTM networks, was employed for the joint angle estimation in both intra- and inter-subject cases. The findings suggest the potential of deep learning methodologies for processing single IMU data to achieve accurate human motion monitoring with fewer sensors in daily life.

To put our study into perspective, a comparison with previous similar data-driven studies conducted by [25], [34], [35], and [40] was made as shown in Table 3. All the previous studies have primarily collected their motion data in a treadmill indoor environment rather than an actual outdoor area. This is a highly controlled data collection motion where subjects have to walk at a certain fixed speed. Walking consistently at the same speed on a treadmill produces a constant walking pattern, unlike overground outdoor walking [47]. Hence, these studies do not represent the natural daily life walking patterns. However, our study was conducted outdoors without any form of guidance or instruction to participants. This puts our study at the forefront of real-world application compared to previous works. Furthermore, all the previous studies have focused only on one motion type, either walking or running. To push the limits of leg joint angle estimation capability from a single inertial sensor, our method investigated four entirely distinct walking patterns. Another criterion is the number of inertial sensors used. It is evident that employing multiple inertial sensors on the lower half of the body enables the estimation of more joint angles and results in higher accuracy. However, this approach is impractical for daily life usage due to the setup time, processing requirements, and inconvenience of wearing multiple sensors. Therefore, the reduction in sensor quantity by leveraging deep learning techniques has garnered recent attention. This paradigm shift from analytical and model-based methods to data-driven joint angle estimation using inertial sensors methods is evident from the four previous studies listed in the table. One common strategy in [25], [35], and [40] is the use of one or two inertial sensors for only one of the leg's joint angles estimation. However, due to the kinematically constrained and rhythmic human locomotion, the other leg's joint angles can be estimated as well. However, the accuracy for the other leg could be lower than the leg with the sensor attached to it. This can be confirmed by our RMSE results in Table 3.

The results of our study suggest a promising future for the use of single inertial sensors in everyday activities. A significant gap between laboratory-controlled settings and real-world applications still exists in this field of study. Therefore, we hope that our study opens new avenues for other researchers to further enhance single-sensor-based biomechanics and gait analysis methods, leading to more practical measurement systems in daily life settings. Consequently, for applications involving instructed straight walking, such as healthcare diagnosis, our study could provide valuable insights into the biomechanics of the lower half of the body with less device attachment to the body of patients. It could also be extended to the development of customized exoskeleton robots attuned to the patient's walking intentions to provide more natural walking assistance. Additionally, due to the simplicity of the system, it could be utilized in the evaluation of surgical outcomes for patients who have undergone leg surgery.

Despite the promising results obtained, the first limitation of this study is it only focused on sagittal plane joint angles of different walking motions and coronal hip joints for sideways walking. Hence, it is only limited to those leg joint angles. As future work, further computations for the frontal and transverse planes, including the ankle joint will be investigated with the addition of other wearable sensor modalities if needed. Another limitation is the demographic limitation of this study. The study has only involved young healthy subjects who do not report any form of mobility impairment recently. Hence, this study cannot generalize to all subjects of different ages and subjects who have any sort of mobility impairment. However, looking at the results of the intra-subject method, personalized systems could work well with subjects of different demography and mobility diseases. Other limitations pertain to the type of motions. Since the sensor is attached to one of the legs, it is assumed that both legs undergo similar movements. If the leg without the sensor makes strange movements completely different from the other, this method could find it hard to estimate the pose of the leg in motion. For complex types of motion such as martial arts, more sensors would be needed on both limbs for accurate estimation. On the other hand, the experimental protocol could be improved as an inertial sensor attached to the foot for ankle joint measurements often produces noisy data due to foot-ground impact. On top of that, there is a risk of the sensor dislodging during high-impact foot-ground interactions. Therefore, future considerations may involve incorporating another low-level sensor, such as an insole sensor, in the foot. The results obtained are currently sufficient for identifying gait events, and this will be expanded to compute essential gait parameters in the future. Such gait parameter calculations will pave the way for implementing a more advanced system applicable to rehabilitation facilities and elderly care centers.

V. CONCLUSION

In summary, this study presents a comprehensive analysis of leg joint angle estimation using a single inertial sensor unit, leveraging the power of Bi-LSTM neural networks. The study was conducted in a real-world outdoor setting,

making it more applicable to daily life scenarios compared to previous studies that primarily used controlled indoor environments for motion data measurement. The predicted results demonstrate a strong correlation with the ground-truth joint angles in both intra- and inter-subject models. Comparatively, the intra-subject model yielded a lower mean absolute error (MAE) compared to the inter-subject model, suggesting the potential for personalized gait analysis. The study expands the scope of motion types to include backward, sideways, zigzag, and ramp walking types, thereby pushing the boundaries of what can be achieved with a single sensor for joint angle estimation. The inter-subject models achieved an RMSE of 4.76°, 4.37°, 5.30°, and 7.09° for the right hip, right knee, left hip, and left knee respectively.

However, the study is not without limitations, such as it focuses on estimating joint angles of a single plane; it only involves young and healthy subjects; it only applies to rhythmic walking activities. Despite these constraints, the findings hold significant promise for various applications, including healthcare diagnosis, development of customized exoskeleton robots, and evaluation of surgical outcomes. The study also opens new avenues for further research, particularly in enhancing single-sensor-based biomechanics and gait analysis methods for more practical measurement systems in daily life settings. Future work will aim to address the current limitations by incorporating additional sensor modalities and expanding the demographic range. Overall, this study serves as a steppingstone towards the practical application of deep learning methodologies in human motion analysis.

REFERENCES

[1] A. Fern'ndez-Baena, A. Susín, and X. Lligadas, "Biomechanical validation of upper-body and lower-body joint movements of Kinect motion capture data for rehabilitation treatments," in *Proc. 4th Int. Conf. Intell. Netw. Collaborative Syst.*, Sep. 2012, pp. 656–661.

[2] P. B. Shull, W. Jirattigalachote, M. A. Hunt, M. R. Cutkosky, and S. L. Delp, "Quantified self and human movement: A review on the clinical impact of wearable sensing and feedback for gait analysis and intervention," *Gait Posture*, vol. 40, no. 1, pp. 11–19, 2014.

[3] P. Ornetti, J. F. Maillefert, D. Laroche, C. Morisset, M. Dougados, and L. Gossec, "Gait analysis as a quantifiable outcome measure in hip or knee osteoarthritis: A systematic review," *Joint Bone Spine*, vol. 77, no. 5, pp. 421–425, 2010, doi: 10.1016/j.jbspin.2009.12.009.

[4] E. Rovini, C. Maremmani, and F. Cavallo, "A wearable system to objectify assessment of motor tasks for supporting Parkinson's disease diagnosis," *Sensors*, vol. 20, no. 9, p. 2630, May 2020, doi: 10.3390/s20092630.

[5] M. M. Churchland, J. P. Cunningham, M. T. Kaufman, J. D. Foster, P. Nuyujukian, S. I. Ryu, and K. V. Shenoy, "Neural population dynamics during reaching," *Nature*, vol. 487, no. 7405, pp. 51–56, Jul. 2012, doi: 10.1038/nature11129.

[6] L. J. Bhargava, M. G. Pandy, and F. C. Anderson, "A phenomenological model for estimating metabolic energy consumption in muscle contraction," *J. Biomech*, vol. 37, no. 1, pp. 81–88, 2004, doi: 10.1016/S0021-9290(03)00239-2.

[7] J. M. Hausdorff, D. A. Rios, and H. K. Edelberg, "Gait variability and fall risk in community-living older adults: A 1-year prospective study," *Arch. Phys. Med. Rehabil.*, vol. 82, no. 8, pp. 1050–1056, Aug. 2001, doi: 10.1053/apmr.2001.24893.

[8] R. Bahr, "Understanding injury mechanisms: A key component of preventing injuries in sport," *Brit. J. Sports Med.*, vol. 39, no. 6, pp. 324–329, Jun. 2005.

[9] S. L. Colyer, M. Evans, D. P. Cosker, and A. I. T. Salo, "A review of the evolution of vision-based motion analysis and the integration of advanced computer vision methods towards developing a markerless system," *Sports Med.-Open*, vol. 4, no. 1, pp. 1–15, Dec. 2018, doi: 10.1186/s40798-018-0139-y.

[10] J. G. Hay and Y. C. Fung, "The biomechanics of sports techniques, 2nd edition," *J. Biomechanical Eng.*, vol. 104, no. 1, p. 73, Feb. 1982, doi: 10.1115/1.3138310.

[11] C. Freeman, T. Exell, K. Meadmore, E. Hallewell, and A. M. Hughes, "Computational models of upper-limb motion during functional reaching tasks for application in FES-based stroke rehabilitation," *Biomed. Tech.*, vol. 60, no. 3, pp. 179–191, Jun. 2015, doi: 10.1515/bmt-2014-0011.

[12] A. B. Zoss, H. Kazerooni, and A. Chu, "Biomechanical design of the Berkeley lower extremity exoskeleton (BLEEX)," *IEEE/ASME Trans. Mechatronics*, vol. 11, no. 2, pp. 128–138, Apr. 2006, doi: 10.1109/TMECH.2006.871087.

[13] K. E. Zelik, S. H. Collins, P. G. Adamczyk, A. D. Segal, G. K. Klute, D. C. Morgenroth, M. E. Hahn, M. S. Orendurff, J. M. Czerniecki, and A. D. Kuo, "Systematic variation of prosthetic foot spring affects center-of-mass mechanics and metabolic cost during walking," *IEEE Trans. Neural Syst. Rehabil. Eng.*, vol. 19, no. 4, pp. 411–419, Aug. 2011, doi: 10.1109/TNSRE.2011.2159018.

[14] S.-R. Ke, L. Zhu, J.-N. Hwang, H.-I. Pai, K.-M. Lan, and C.-P. Liao, "Real-time 3D human pose estimation from monocular view with applications to event detection and video gaming," in *Proc. 7th IEEE Int. Conf. Adv. Video Signal Based Surveill.*, Sep. 2010, pp. 489–496, doi: 10.1109/AVSS.2010.80.

[15] H.-S. Fang, J. Li, H. Tang, C. Xu, H. Zhu, Y. Xiu, Y.-L. Li, and C. Lu, "AlphaPose: Whole-body regional multi-person pose estimation and tracking in real-time," *IEEE Trans. Pattern Anal. Mach. Intell.*, vol. 45, no. 6, pp. 7157–7173, Jun. 2023, doi: 10.1109/TPAMI.2022.3222784.

[16] A. Mathis, P. Mamidanna, K. M. Cury, T. Abe, V. N. Murthy, M. W. Mathis, and M. Bethge, "DeepLabCut: Markerless pose estimation of user-defined body parts with deep learning," *Nature Neurosci.*, vol. 21, no. 9, pp. 1281–1289, Sep. 2018, doi: 10.1038/s41593-018-0209-y.

[17] Z. Cao, G. Hidalgo, T. Simon, S.-E. Wei, and Y. Sheikh, "OpenPose: Realtime multi-person 2D pose estimation using part affinity fields," *IEEE Trans. Pattern Anal. Mach. Intell.*, vol. 43, no. 1, pp. 172–186, Jan. 2021, doi: 10.1109/TPAMI.2019.2929257.

[18] T. Tadesse Alemayoh, J. Hoon Lee, and S. Okamoto, "LocoESIS: Deep-learning-based leg-joint angle estimation from a single pelvis inertial sensor," in *Proc. 9th IEEE RAS/EMBS Int. Conf. Biomed. Robot. Biomechatronics (BioRob)*, Aug. 2022, pp. 01–07, doi: 10.1109/BioRob52689.2022.9925420.

[19] D. Kobsar, Z. Masood, H. Khan, N. Khalil, M. Y. Kiwan, S. Ridd, and M. Tobis, "Wearable inertial sensors for gait analysis in adults with osteoarthritis—A scoping review," *Sensors*, vol. 20, no. 24, p. 7143, Dec. 2020, doi: 10.3390/s20247143.

[20] J. Favre, B. M. Jolles, O. Siegrist, and K. Aminian, "Quaternion-based fusion of gyroscopes and accelerometers to improve 3D angle measurement," *Electron. Lett.*, vol. 42, no. 11, p. 612, 2006, doi: 10.1049/el:20060124.

[21] M. Topley and J. G. Richards, "A comparison of currently available optoelectronic motion capture systems," *J. Biomechanics*, vol. 106, Jun. 2020, Art. no. 109820, doi: 10.1016/j.jbiomech.2020.109820.

[22] N. Seethapathi, S. Wang, R. Saluja, G. Blohm, and K. P. Kording, "Movement science needs different pose tracking algorithms," 2019, *arXiv:1907.10226*.

[23] Y. Luo, Y. Li, M. Foshey, W. Shou, P. Sharma, T. Palacios, A. Torralba, and W. Matusik, "Intelligent carpet: Inferring 3D human pose from tactile signals," in *Proc. IEEE/CVF Conf. Comput. Vis. Pattern Recognit. (CVPR)*, Jun. 2021, pp. 11250–11260, doi: 10.1109/CVPR46437.2021.01110.

[24] S. Sivakumar, A. A. Gopalai, K. H. Lim, D. Gouwanda, and S. Chauhan, "Joint angle estimation with wavelet neural networks," *Sci. Rep.*, vol. 11, no. 1, p. 10306, May 2021, doi: 10.1038/s41598-021-89580-y.

[25] M. Gholami, C. Napier, and C. Menon, "Estimating lower extremity running gait kinematics with a single accelerometer: A deep learning approach," *Sensors*, vol. 20, no. 10, p. 2939, May 2020, doi: 10.3390/s20102939.

[26] M. Mundt, A. Koeppe, S. David, T. Witter, F. Bamer, W. Potthast, and B. Markert, "Estimation of gait mechanics based on simulated and measured IMU data using an artificial neural network," *Frontiers Bioeng. Biotechnol.*, vol. 8, p. 41, Feb. 2020, doi: 10.3389/fbioe.2020.00041.

[27] T. T. Alemayoh, J. H. Lee, and S. Okamoto, "Leg-joint angle estimation from a single inertial sensor attached to various lower-body links during walking motion," *Appl. Sci.*, vol. 13, no. 8, p. 4794, Apr. 2023, doi: 10.3390/app13084794.
[28] F. Wouda, M. Giuberti, G. Bellusci, and P. Veltink, "Estimation of full-body poses using only five inertial sensors: An eager or lazy learning approach?" *Sensors*, vol. 16, no. 12, p. 2138, Dec. 2016, doi: 10.3390/s16122138.
[29] J. Wang, Y. Dai, and X. Si, "Analysis and recognition of human lower limb motions based on electromyography (EMG) signals," *Electronics*, vol. 10, no. 20, p. 2473, Oct. 2021, doi: 10.3390/electronics10202473.
[30] Y. Deng, F. Gao, and H. Chen, "Angle estimation for knee joint movement based on PCA-RELM algorithm," *Symmetry*, vol. 12, no. 1, p. 130, Jan. 2020, doi: 10.3390/sym12010130.
[31] S. Subramaniam, S. Majumder, A. I. Faisal, and M. J. Deen, "Insole-based systems for health monitoring: Current solutions and research challenges," *Sensors*, vol. 22, no. 2, p. 438, Jan. 2022, doi: 10.3390/s22020438.
[32] P. Picerno, "25 years of lower limb joint kinematics by using inertial and magnetic sensors: A review of methodological approaches," *Gait Posture*, vol. 51, pp. 239–246, Jan. 2017, doi: 10.1016/j.gaitpost.2016.11.008.
[33] H. Dejnabadi, B. M. Jolles, and K. Aminian, "A new approach to accurate measurement of uniaxial joint angles based on a combination of accelerometers and gyroscopes," *IEEE Trans. Biomed. Eng.*, vol. 52, no. 8, pp. 1478–1484, Aug. 2005, doi: 10.1109/TBME.2005.851475.
[34] F. J. Wouda, M. Giuberti, G. Bellusci, E. Maartens, J. Reenalda, B.-J.-F. van Beijnum, and P. H. Veltink, "Estimation of vertical ground reaction forces and sagittal knee kinematics during running using three inertial sensors," *Frontiers Physiol.*, vol. 9, p. 218, Mar. 2018, doi: 10.3389/fphys.2018.00218.
[35] T. Lee, I. Kim, and S.-H. Lee, "Estimation of the continuous walking angle of knee and ankle (talocrural joint, subtalar joint) of a lower-limb exoskeleton robot using a neural network," *Sensors*, vol. 21, no. 8, p. 2807, Apr. 2021, doi: 10.3390/s21082807.
[36] S. Wang, Y. Cai, K. Hase, K. Uchida, D. Kondo, T. Saitou, and S. Ota, "Estimation of knee joint angle during gait cycle using inertial measurement unit sensors: A method of sensor-to-clinical bone calibration on the lower limb skeletal model," *J. Biomechanical Sci. Eng.*, vol. 17, no. 1, p. 00196, 2022, doi: 10.1299/JBSE.21-00196.
[37] T. Seel, J. Raisch, and T. Schauer, "IMU-based joint angle measurement for gait analysis," *Sensors*, vol. 14, no. 4, pp. 6891–6909, Apr. 2014, doi: 10.3390/s140406891.
[38] T. F. de Almeida, E. Morya, A. C. Rodrigues, and A. F. O. de Azevedo Dantas, "Development of a low-cost open-source measurement system for joint angle estimation," *Sensors*, vol. 21, no. 19, p. 6477, Sep. 2021, doi: 10.3390/s21196477.
[39] C. Woods and V. Vikas, "Joint angle estimation using accelerometer arrays and model-based filtering," *IEEE Sensors J.*, vol. 22, no. 20, pp. 19786–19796, Oct. 2022, doi: 10.1109/JSEN.2022.3200251.
[40] J. Sung, S. Han, H. Park, H.-M. Cho, S. Hwang, J. W. Park, and I. Youn, "Prediction of lower extremity multi-joint angles during overground walking by using a single IMU with a low frequency based on an LSTM recurrent neural network," *Sensors*, vol. 22, no. 1, p. 53, Dec. 2021, doi: 10.3390/s22010053.
[41] M. Schepers, M. Giuberti, and G. Bellusci, "Xsens MVN: Consistent tracking of human motion using inertial sensing," *Xsens Technol.*, vol. 1, no. 8, pp. 1–8, 2018.
[42] J.-T. Zhang, A. C. Novak, B. Brouwer, and Q. Li, "Concurrent validation of Xsens MVN measurement of lower limb joint angular kinematics," *Physiological Meas.*, vol. 34, no. 8, pp. 63–69, Aug. 2013, doi: 10.1088/0967-3334/34/8/N63.
[43] M. Schuster and K. K. Paliwal, "Bidirectional recurrent neural networks," *IEEE Trans. Signal Process.*, vol. 45, no. 11, pp. 2673–2681, Nov. 1997, doi: 10.1109/78.650093.
[44] S. Hochreiter and J. Schmidhuber, "Long short-term memory," *Neural Comput.*, vol. 9, no. 8, pp. 1735–1780, Nov. 1997, doi: 10.1162/neco.1997.9.8.1735.
[45] A. Graves and J. Schmidhuber, "Framewise phoneme classification with bidirectional LSTM and other neural network architectures," *Neural Netw.*, vol. 18, nos. 5–6, pp. 602–610, Jul. 2005, doi: 10.1016/j.neunet.2005.06.042.
[46] P. J. Huber, "Robust estimation of a location parameter," *Ann. Math. Statist.*, vol. 35, no. 1, pp. 73–101, Mar. 1964, doi: 10.1214/aoms/1177703732.
[47] S. J. Lee and J. Hidler, "Biomechanics of overground vs. treadmill walking in healthy individuals," *J. Appl. Physiol.*, vol. 104, no. 3, pp. 747–755, Mar. 2008, doi: 10.1152/japplphysiol.01380.2006.

TSIGE TADESSE ALEMAYOH (Student Member, IEEE) received the B.S. degree in electrical and electronics engineering from Mekelle University, Ethiopia, and the M.Engg. degree in mechanical engineering from Ehime University, Japan, where he is currently pursuing the Ph.D. degree with the Department of Mechanical Engineering.

From 2016 to 2017, he was an Assistant Lecturer with Mekelle University.

Mr. Alemayoh has been a Regular Member of the Japanese Society of Mechanical Engineers (JSME), since 2021.

JAE HOON LEE (Member, IEEE) received the B.S. degree in mechanical and automatic control engineering from the Korea University of Technology and Education, in 1996, and the M.S. and Ph.D. degrees in electric, electrical, control and instrumentation engineering from Hanyang University, South Korea, in 1998 and 2003, respectively.

From 2004 to 2006, he was a Postdoctoral Fellow with the Intelligent Robot Laboratory, University of Tsukuba, Japan. From 2007 to 2008, he was a JSPS Fellow with the Ubiquitous Functions Research Group, Intelligent Systems Research Institute, AIST, Japan. He is currently a Professor with the Department of Mechanical Engineering, Graduate School of Science and Engineering, Ehime University, Japan. He is the author of more than 150 articles. His research interests include deep learning-based human motion recognition, gait assessment using wearable sensors, development of drone system for inspection tasks, biped walking robot, parallel mechanism using variable stiffness actuators, and industrial applications of deep learning.

Dr. Lee was a recipient of the Best Application Paper from the 18th International Conference on Ubiquitous Robots and Ambient Intelligence (URAI), in 2021, and the Best Paper Award from the 18th International Symposium on Artificial Life and Robotics (AROB), in 2013.

SHINGO OKAMOTO received the B.S. and M.S. degrees in engineering from Ehime University, Japan, in 1982 and 1984, respectively, and the Ph.D. degree in engineering from the Tokyo Institute of Technology, Japan, in 1992.

He has been doing researches as a Researcher with the Research and Development Center, Toshiba Corporation, since 1984. Since 1992, he has been a Research Associate. Since 1994, he has been an Associate Professor with Hiroshima University, Japan. From 1998 to 1999, he had been doing a research as a Visiting Scientist with the Prof. K. J. Bathe in Massachusetts Institute of Technology. Since 2008, he has been a Professor of mechanical engineering course with Ehime University. His research interests include robotics, intelligent systems, artificial intelligence, biomedical engineering science, and computational mechanics.

Dr. Okamoto received the Best Paper Award from the International Conference on Engineering & Technology, Computer, Basic & Applied Science (ECBA) in the field of biomedical engineering science and the Technology Prize from the Society of Instrument and Control Engineers (SICE), in 2016.